



## Chemo-enzymatic phenol polymerisation via in-situ H<sub>2</sub>O<sub>2</sub> synthesis

Liwei Zhang<sup>a,b,1</sup>, Richard J. Lewis<sup>b,\*,1</sup>, Joseph Brehm<sup>b</sup>, Wencong Liu<sup>a</sup>, David J. Morgan<sup>b,c</sup>, Thomas E. Davies<sup>b</sup>, Yong Wang<sup>a</sup>, Graham J. Hutchings<sup>b,\*</sup>

<sup>a</sup> Advanced Materials and Catalysis Group, Center of Chemistry for Frontier Technologies, State Key Laboratory of Clean Energy Utilization, Institute of Catalysis, Department of Chemistry, Zhejiang University, Hangzhou 310058, PR China

<sup>b</sup> Max Planck, Cardiff Centre on the Fundamentals of Heterogeneous Catalysis FUNCAT, Cardiff Catalysis Institute, School of Chemistry, Cardiff University, Cardiff CF24 4HQ, United Kingdom

<sup>c</sup> HarwellXPS, Research Complex at Harwell (RCAH), Didcot OX11 0FA, United Kingdom

### ARTICLE INFO

#### Keywords:

Chemo-enzymatic cascade  
Hydrogen peroxide  
AuPd  
Horseradish peroxidase  
Phenol

### ABSTRACT

Within this contribution, the combination of supported AuPd nanoalloys with horseradish peroxidase is demonstrated to offer high efficacy towards the one-pot oxidative polymerisation of the model wastewater contaminant phenol, via the chemo-catalytic supply of in-situ generated H<sub>2</sub>O<sub>2</sub>. Notably, the utilisation of AuPd alloyed formulations offered considerably improved cascade efficiencies, compared to that observed over monometallic analogues, with the optimal 0.5%Au-0.5%Pd/TiO<sub>2</sub> catalyst achieving total conversion of phenol within 15 minutes when used in conjunction with the enzyme. Importantly, the in-situ chemo-enzymatic system was shown to offer good stability over successive reactions, and outperforms analogous approaches reliant on the use of preformed H<sub>2</sub>O<sub>2</sub>, while also avoiding the proprietary stabilising agents present in the commercial oxidant.

### 1. Introduction

The presence of phenolic compounds, stemming from polymer processing, oil refining and fibre/textile manufacture, in water bodies represents a growing risk to aquatic and human health. As with many organic compounds found in industrial waste streams, conventional water treatment processes offer only a limited efficacy towards the degradation of phenols and as such a significant reliance is placed on the use of carbon beds to remove these pollutants through adsorption. These beds, are ultimately incinerated or taken to landfill, where pollutants can be released back into the environment (as CO<sub>2</sub> in the case of incineration). Alternatively, advanced oxidation processes (AOPs), which utilise oxygen-based radicals that are generated through the combination of preformed H<sub>2</sub>O<sub>2</sub> with O-Zone (H<sub>2</sub>O<sub>2</sub>/O<sub>3</sub>) or ultraviolet light (H<sub>2</sub>O<sub>2</sub>/UV), are promising routes to recalcitrant remediation. However, high costs associated with the reagents or light sources and the complexity of their operation may hinder large-scale adoption. Alternative catalytic processes have also been reported, which synthesize identical reactive oxygen species to those generated via AOPs[1,2]. However, such total-oxidation approaches also suffer from the need to fully mineralise the contaminant, with partial oxidation by-products,

such as catechol, hydroquinone or oxalic, maleic and fumaric acids, in the case of phenol, posing significant health risks. Indeed, as is the case with a range of chemical pollutants the health risks, posed by partially oxidised phenolic intermediates are greater than that of phenol itself.

The coupling of H<sub>2</sub>O<sub>2</sub> generated in-situ over chemo-catalysts, with enzymes for oxidative transformations has recently been reported and represents an attractive alternative to more traditional approaches which have typically relied on multi-enzyme cascades to produce the feedstock oxidant[3,4]. Indeed, the supply of H<sub>2</sub>O<sub>2</sub> through the use of glucose oxidase (GO<sub>x</sub>), formate oxidase (FO<sub>x</sub>) or choline oxidase (ChO<sub>x</sub>) co-enzymes, suffers from poor atom efficiency and the formation of stoichiometric quantities of undesirable by-products[5–8]. Alternatively, the continual introduction of pre-formed aqueous solutions of H<sub>2</sub>O<sub>2</sub> (i.e. that generated ex-situ), leads to excessive dilution of product streams, the generation of H<sub>2</sub>O<sub>2</sub> hot-spots (i.e. areas of high H<sub>2</sub>O<sub>2</sub> concentrations within the reactor, which can lead to enzyme deactivation), poor utilisation of the oxidant due to H<sub>2</sub>O formation, and significant safety concerns[9]. We have recently reported the effective coupling of in-situ H<sub>2</sub>O<sub>2</sub> generation, over supported AuPd nanoalloys, with the evolved unspecific peroxygenase (UPO), referred to as PaDa-I, for the selective oxidation of a range of C-H bonds, facilitating the formation of

\* Corresponding authors.

E-mail addresses: [LewisR27@Cardiff.ac.uk](mailto:LewisR27@Cardiff.ac.uk) (R.J. Lewis), [Hutch@Cardiff.ac.uk](mailto:Hutch@Cardiff.ac.uk) (G.J. Hutchings).

<sup>1</sup> These authors contributed equally to this work

hydroxylated products[10]. In doing so it has been possible to bridge the wide conditions gap that exists between H<sub>2</sub>O<sub>2</sub> direct synthesis (favoured by elevated pressures (typically 10–40 bar), sub-ambient temperatures (typically 0–10 °C) and acidic or halide promoters (typically [H<sup>+</sup>] = 0.4 M and [X<sup>-</sup>] = 0.01 M), [11] and enzymatic stability, which typically requires near ambient temperatures, pressures and a near-neutral pH.

Horseradish peroxxygenase (HRP), a well-studied and commercially available oxidoreductase enzyme has been shown to be highly effective in the removal of a wide variety of aromatic compounds[12–14], through the formation of water-insoluble polymers, when coupled with H<sub>2</sub>O<sub>2</sub>. In particular, the oxidative polymerisation of phenol and its derivatives has received significant interest[15,16], with the polymerisation mechanism suggested to proceed through (i) a H<sub>2</sub>O<sub>2</sub>-mediated two-electron transfer from the Fe<sup>3+</sup> active site residue within HRP, (ii) two successive one-electron donations from the phenolic substrate to the HRP Fe-centre, resulting in the formation of two phenoxy radicals which (iii) ultimately react to form a dimeric product, which may then participate in further coupling cycles to yield higher order oligomers [17]. However, as with other enzymatic transformations reliant on H<sub>2</sub>O<sub>2</sub>, concerns associated with atom efficiency or the presence of toxic stabilising agents when utilising the preformed oxidant, have prevented adoption at scale.

With these earlier works in mind, within this contribution we highlight the efficacy of a coupled chemo-catalytic/enzymatic approach to phenol remediation, utilising supported AuPd nanoalloys, which are amongst the state-of-the-art for H<sub>2</sub>O<sub>2</sub> direct synthesis[18,19], and the enzyme horseradish peroxxygenase.

## 2. Experimental

### 2.1. Catalyst synthesis

Mono- and bi-metallic 1 %AuPd/TiO<sub>2</sub> catalysts have been prepared (on a weight basis) via a conventional wet co-impregnation procedure, based on a methodology previously reported in the literature[20]. The procedure to produce the 0.5 %Au–0.5 %Pd/TiO<sub>2</sub> catalyst (2 g) is outlined below, with a similar methodology utilized for all formulations.

Aqueous solutions of PdCl<sub>2</sub> (1.25 mL, [Pd] = 8.0 mgmL<sup>-1</sup>, Merck) and HAuCl<sub>4</sub>·3 H<sub>2</sub>O (0.807 mL, [Au] = 12.4 mgmL<sup>-1</sup>, Strem Chemicals) were mixed in a 50 mL round-bottom flask and heated to 65 °C with stirring (1000 rpm) in a thermostatically controlled oil bath, with total volume fixed to 16 mL using H<sub>2</sub>O (HPLC grade, Fischer Scientific). Upon reaching 65 °C, TiO<sub>2</sub> (1.98 g, Degussa, P25) was added over the course of 5 min with constant stirring. The resulting slurry was stirred at 65 °C for a further 15 min, following this the temperature was raised to 95 °C for 16 h to allow for complete evaporation of water. The resulting solid was ground prior to an oxidative heat treatment (flowing air, 400 °C, 3 h, 10 °C min<sup>-1</sup>).

Surface area measurements of key catalytic materials, as determined by five-point N<sub>2</sub> adsorption are reported in Table S.1. Corresponding analysis by X-ray diffraction is reported in Figure S.1, with no reflections associated with immobilised metals observed, which may be indicative of the high dispersion of metal species. Finally, SEM analysis of the catalyst series is reported in Figure S.2, with the metal nanoparticles found to be poorly distributed on the catalyst support, which may be expected given the impregnation route to catalyst synthesis[21].

### 2.2. Catalyst testing

**Note 1:** In all cases, reactions were run multiple times (a minimum of three), over multiple batches of catalyst (a minimum of two), with the data being presented as an average of these experiments for clarity. In the case of the chemo-catalytic H<sub>2</sub>O<sub>2</sub> synthesis experiments the standard error was found to be between 2 % and 4 %, while in the case of the chemo-enzymatic polymerisation of phenol the standard error was found to be between 2 % and 5 %.

**Note 2:** Reaction conditions used within this study operate outside the flammability limits of gaseous mixtures of H<sub>2</sub> and O<sub>2</sub>.

### 2.3. Direct synthesis of H<sub>2</sub>O<sub>2</sub> from H<sub>2</sub> and O<sub>2</sub>

Reactions were carried out in 50 mL gas-tight round-bottomed flasks rated to 60 psi and stirred using a Radleys 6 Plus Carousel equipped with a gas distribution system. The catalyst (0.001 g) was weighed directly into the glass flasks. To this was added potassium phosphate buffer (10 mL of 100 mM, pH 6.0) prepared with KH<sub>2</sub>PO<sub>4</sub> and K<sub>2</sub>HPO<sub>4</sub> (both obtained from Merck). Subsequently, the flask was sealed and pressurized to 29 psi with H<sub>2</sub> (23 psi) and air (6 psi) to give a reaction atmosphere containing 80 % H<sub>2</sub> and 20 % air. The reaction mixtures were stirred (250 rpm) at ambient temperature (20 °C) for 0.5 h, unless otherwise stated. After the desired reaction time the vessel was depressurized and the H<sub>2</sub>O<sub>2</sub> concentration was determined by UV/Vis spectroscopy. To determine H<sub>2</sub>O<sub>2</sub> concentration an aliquot (1.5 mL) of the post-reaction solution was combined with potassium titanium oxalate dihydrate solution acidified with 30 % H<sub>2</sub>SO<sub>4</sub> (0.02 M, 1.5 mL) resulting in the formation of an orange perititanic acid complex. This resulting solution was analysed spectrophotometrically using an Agilent Cary 60 UV/Vis Spectrophotometer at 400 nm by comparison to a calibration curve by taking aliquots of H<sub>2</sub>O<sub>2</sub> in the buffer solution (1.5 mL) and adding acidified potassium titanium oxalate dihydrate solution (1.5 mL).

Additional H<sub>2</sub>O<sub>2</sub> synthesis experiments were conducted in the presence of HRP (4 U mL<sup>-1</sup>), with all other reaction conditions as outlined above.

### 2.4. Degradation of H<sub>2</sub>O<sub>2</sub>

Catalytic activity towards H<sub>2</sub>O<sub>2</sub> degradation (via hydrogenation and decomposition pathways) was determined in a similar manner to that used to measure the direct synthesis activity of a catalyst. The potassium phosphate buffer (10 mL of 100 mM, pH6.0) prepared with KH<sub>2</sub>PO<sub>4</sub> and K<sub>2</sub>HPO<sub>4</sub> (both obtained from Merck) and H<sub>2</sub>O<sub>2</sub> (2000ppm, Merck) were added into the 50 mL gas-tight round-bottomed flasks. From the solution, prior to the addition of the catalyst, two 0.05 g aliquots were removed to allow for the quantification of the initial H<sub>2</sub>O<sub>2</sub> concentration via UV/Vis spectroscopy. Subsequently, the catalyst (0.001 g) was added to the flask, which was then sealed, purged and pressurized to 29 psi with H<sub>2</sub> (23 psi) and N<sub>2</sub> (6 psi) to give a reaction atmosphere containing 80 % H<sub>2</sub> and 20 % N<sub>2</sub>. The reaction mixtures were stirred (250 rpm) at ambient temperature (20 °C) for the desired reaction time. Subsequently, the vessel was depressurized, the catalyst was removed via filtration and the remaining H<sub>2</sub>O<sub>2</sub> was quantified by UV/Vis spectroscopy, as outlined above.

Additional studies were conducted, in the absence of the chemo-catalyst and presence of HRP (2–10 U mL<sup>-1</sup>) to probe the enzymatic contribution to H<sub>2</sub>O<sub>2</sub> degradation, with total pressure maintained at 29 psi using N<sub>2</sub> and a H<sub>2</sub>O<sub>2</sub> concentration of 50 ppm and all other reaction conditions as outlined above.

### 2.5. Metal leaching studies

To provide an indication of the extent of metal leaching during the in-situ phenol polymerisation reaction, indicative model studies were conducted in the absence of the enzyme and substrate (i.e. under H<sub>2</sub>O<sub>2</sub> direct synthesis conditions) utilising 0.01 g of the heterogeneous catalyst (i.e. ten times that utilised for the direct synthesis and phenol polymerisation reactions), with all other conditions as outlined as above. Post-reaction, the chemo-catalyst was removed via filtration and the reaction solution was analysed by ICP-MS.

## 2.6. Horseradish peroxidase (HRP) preparation

Enzyme activities were determined using ABTS (2,2'-Azinobis-(3-Ethylbenzthiazolin-6-Sulfonic Acid), as substrate. Reactions were run in triplicate, 20  $\mu\text{L}$  HRP (type VI, Sigma-Aldrich) was added to 180  $\mu\text{L}$  ABTS reaction mixture (100 mM sodium citrate-phosphate pH 6 with 0.3 mM ABTS and 2 mM  $\text{H}_2\text{O}_2$ ) and substrate conversion was followed by measuring the absorption at 418 nm ( $\epsilon_{418} = 31,100 \text{ M}^{-1} \text{ cm}^{-1}$ ). The HRP concentration was appropriately diluted to give rise to linear enzyme kinetics. One unit is defined as the amount of enzyme that converts 1  $\mu\text{mol}$  of substrate in 1 min.

## 2.7. Chemo-enzymatic phenol polymerisation

Reactions were carried out in 50 mL gas-tight round-bottomed flasks rated to 60 psi and stirred using a Radleys 6 Plus Carousel equipped with a gas distribution system. The reaction mixtures contained 4  $\text{U mL}_{\text{RM}}^{-1}$  HRP (type VI, Sigma-Aldrich), 0.1  $\text{mg mL}_{\text{RM}}^{-1}$  of the metal catalyst (0.001 g) in potassium phosphate buffer (10 mL, 100 mM, pH 6, Merck) and phenol (0.3 mM, Sigma-Aldrich). The catalysts were weighed directly into the glass vessels followed by the buffer solution. Immediately before starting the reactions, the enzyme and substrate were added. The sealed reaction vessels were pressurised to 29 psi with  $\text{H}_2$  (23 psi) and air (6 psi) to give a reaction atmosphere containing 80 %  $\text{H}_2$  and 20 % air. The reactions were stirred with a magnetic stirrer bar at 250 rpm at ambient temperature (20  $^\circ\text{C}$ ) for the desired reaction time, typically 1.5 h. After the desired reaction time product formation was monitored by HPLC analysis (Agilent 1200 series, equipped with Poroshell-120, EC-C18 column). We highlight to the reader that it was not possible for full quantification of polymeric products, and as such only the extent of phenol polymerisation is reported.

Phenol polymerisation was determined as follows:

$$\text{Phenol polymerisation (\%)} = \frac{\text{mmol}_{\text{phenol}(t(0))} - \text{mmol}_{\text{phenol}(t(1))}}{\text{mmol}_{\text{phenol}(t(0))}} \times 100 \quad (1)$$

Residual  $\text{H}_2\text{O}_2$ , generated chemo-catalytically, was measured via UV/Vis as outlined above. In the case of our chemo-enzymatic experiments, we were unable to detect any  $\text{H}_2\text{O}_2$  in post-reaction solutions, which may indicate the increased rate of  $\text{H}_2\text{O}_2$  utilisation, compared to  $\text{H}_2\text{O}_2$  supply. However, one must also consider the contribution from competitive  $\text{H}_2\text{O}_2$  degradation pathways, particularly given the poor stability of  $\text{H}_2\text{O}_2$  under ambient temperatures.

Further in-situ oxidation studies were carried out to determine the efficacy of using pre-formed  $\text{H}_2\text{O}_2$ , at levels identical to those over a range of  $\text{H}_2\text{O}_2$  concentrations (20–100 ppm), under identical conditions to those used above for in-situ chemo-enzymatic phenol polymerisation, with total pressure fixed to 29 psi with  $\text{N}_2$ . Additional studies were conducted under individual gaseous reagents ( $\text{H}_2$  and  $\text{O}_2$  as air), with total pressure maintained at 29 psi with  $\text{N}_2$ .

Based on the time-on-line data presented in Fig. 1.B, which demonstrated that total phenol conversion may be achieved (over the 0.5 %Au-0.5 %Pd/ $\text{TiO}_2$  catalyst), at a reaction time of 15 minutes. Additional experiments were conducted to probe the stability of the chemo-enzymatic system over successive phenol polymerisation experiments, using the optimal 0.5 %Au-0.5 %Pd/ $\text{TiO}_2$  catalyst (0.001 g) and 4  $\text{U mL}_{\text{RM}}^{-1}$  HRP (type VI, Sigma-Aldrich). After achieving total phenol conversion, the system was depressurised and additional substrate (phenol, 0.3 mM, Sigma-Aldrich) and gaseous reagents  $\text{H}_2$  (23 psi) and air (6 psi) were introduced into the reactor. The reaction was then allowed to proceed to complete phenol polymerisation, before reagents were recharged as outlined above.

## 2.8. Catalyst reusability in the tandem chemo-enzymatic polymerisation of phenol and chemo-catalytic direct synthesis of $\text{H}_2\text{O}_2$

The performance of key chemo-catalytic formulations was evaluated over multiple uses towards both the direct synthesis of  $\text{H}_2\text{O}_2$  and phenol polymerisation, when used in combination with the HRP enzyme. To obtain sufficient catalyst samples for testing over multiple uses, model  $\text{H}_2\text{O}_2$  synthesis reactions containing 0.05 g of chemo-catalyst were initially conducted. The spent catalyst was collected by vacuum filtration and washed with potassium phosphate buffer (2  $\times$  5 mL, pH6, 100 mM), before drying under vacuum (30  $^\circ\text{C}$ , 16 h). Aliquots of the dried sample (0.001 g) were then separately evaluated for activity towards  $\text{H}_2\text{O}_2$  direct synthesis and in-situ polymerisation of phenol. The procedure described above was repeated to allow for the evaluation of the chemo-catalyst upon successive uses.

## 2.9. Characterisation

Brunauer Emmett Teller (BET) surface area measurements were conducted using a Quadrasorb surface area analyser. A 5-point isotherm of each material was measured using  $\text{N}_2$  as the adsorbate gas. Samples were degassed at 250  $^\circ\text{C}$  for 2 h prior to the surface area being determined by 5-point  $\text{N}_2$  adsorption at  $-196$   $^\circ\text{C}$ , and data analysed using the BET method.

The bulk structure of the catalysts was determined by powder X-ray diffraction using a (0-0) PANalytical X'pert Pro powder diffractometer using a  $\text{Cu K}\alpha$  radiation source, operating at 40 KeV and 40 mA. Standard analysis was carried out using a 40 min run with a back filled sample, between  $2\theta$  values of 10 – 80  $^\circ$ . Phase identification was carried out using the International Centre for Diffraction Data (ICDD).

A Thermo Scientific K-Alpha<sup>+</sup> photoelectron spectrometer was used to collect XP spectra utilising a micro-focused monochromatic Al  $\text{K}\alpha$  X-ray source operating at 72 W. Data was collected over an elliptical area of approximately 400  $\mu\text{m}^2$  at pass energies of 40 and 150 eV for high-resolution and survey spectra, respectively. Sample charging effects were minimised through a combination of low-energy electrons and  $\text{Ar}^+$  ions, consequently this resulted in a C(1 s) line at 284.8 eV for all samples. All data was processed using CasaXPS v2.3.24 using a Shirley background, Scofield sensitivity factors and an electron energy dependence of  $-0.6$  as recommended by the manufacturer.

SEM analysis was performed using a TESCAN MAIA3 microscope operating at 5–30kV. Samples were mounted on 12.5 mm aluminium stubs using adhesive carbon tabs and analysed uncoated.

Metal leaching was quantified using an Agilent 7900 ICP-MS equipped with an I-AS auto-sampler using a 5-point calibration using certified reference materials from Perkin Elmer and certified internal standards from Agilent. All calibrants were matrix matched.

## 3. Results and discussion

Our initial studies established the efficacy of a range of supported AuPd chemo-catalysts, prepared by a wet co-impregnation procedure, towards the direct synthesis of  $\text{H}_2\text{O}_2$ , under reaction conditions that we have previously demonstrated to be suitable for enzymatic stability, namely under ambient temperatures (20  $^\circ\text{C}$ ), low pressure (29 psi) and using a phosphate-buffered reaction medium (pH6)[3,22]. Catalytic performance as a function of reaction time (up to 2 h) is reported in Fig. S3, with  $\text{H}_2\text{O}_2$  synthesis rates after a reaction time of 5 and 120 min reported in Table 1. Notably, we have previously demonstrated that the initial rate of chemo-catalytic  $\text{H}_2\text{O}_2$  synthesis (*i.e.*  $\text{H}_2\text{O}_2$  production rates at reaction times where the contribution from competitive  $\text{H}_2\text{O}_2$  degradation can be ignored and the reaction can be considered to not be limited by reagent availability), is a reasonable predictor of the performance of the chemo-enzymatic system as a whole[23]. Here, it is important to note that while the initial rate of chemo-catalytic  $\text{H}_2\text{O}_2$  synthesis can indicate cascade performance, there is a potential for

**Table 1**

Comparison of catalytic activity towards the direct synthesis of H<sub>2</sub>O<sub>2</sub>, under low-pressure conditions.

Catalyst	H <sub>2</sub> O <sub>2</sub> Concentration / ppm (mM)		Reaction Rate / mmol <sub>H<sub>2</sub>O<sub>2</sub></sub> mmol <sub>metal</sub> <sup>-1</sup> h <sup>-1</sup>	
	5 min	120 min	5 min	120 min
1 %Au/TiO <sub>2</sub>	1 (0.03)	8 (0.24)	6.94 × 10 <sup>1</sup>	2.31 × 10 <sup>1</sup>
0.75 %Au–0.25 %Pd/TiO <sub>2</sub>	5 (0.15)	47 (1.38)	2.86 × 10 <sup>2</sup>	1.12 × 10 <sup>2</sup>
0.5 %Au–0.5 %Pd/TiO <sub>2</sub>	21 (0.62)	89 (2.62)	1.02 × 10 <sup>3</sup>	1.81 × 10 <sup>2</sup>
0.25 %Au–0.75 %Pd/TiO <sub>2</sub>	18 (0.53)	29 (0.85)	7.63 × 10 <sup>2</sup>	5.12 × 10 <sup>1</sup>
1 %Pd/TiO <sub>2</sub>	6 (0.18)	10 (0.29)	2.25 × 10 <sup>2</sup>	1.56 × 10 <sup>1</sup>

H<sub>2</sub>O<sub>2</sub> direct synthesis reaction conditions: Catalyst (0.001 g), phosphate buffer (100 mM, 10 mL, pH 6.0), using a gas mixture of 80 % H<sub>2</sub>/air (23 psi H<sub>2</sub>, 6 psi air), 20 °C, 250 rpm.

deviation away from this correlation if there are changes in active site composition or structure. For example, such variation may result from exposure of the chemo-catalyst to reaction conditions or through interaction with cascade reaction products, and can alter chemo-catalytic H<sub>2</sub>O<sub>2</sub> synthesis rates. This is particularly important in the case of in-situ H<sub>2</sub>O<sub>2</sub>-mediated transformations, where the reduction of Pd species can result from exposure to a H<sub>2</sub>-rich atmosphere. We also highlight the additional caveat that H<sub>2</sub>O<sub>2</sub> production rate can only indicate cascade performance when the rate of enzymatic H<sub>2</sub>O<sub>2</sub> utilisation exceeds that of H<sub>2</sub>O<sub>2</sub> synthesis (*i.e.* where the reaction is limited by the supply of the oxidant).

In keeping with earlier studies[24] the alloying of Au with Pd was found to offer significant improvements in catalytic activity, compared to that of monometallic analogues, with the performance of the 0.5 % Au–0.5 %Pd/TiO<sub>2</sub> formulation (1.02 × 10<sup>3</sup> mmol<sub>H<sub>2</sub>O<sub>2</sub></sub>mmol<sub>metal</sub><sup>-1</sup>h<sup>-1</sup> at a reaction time of 5 minutes), particularly notable.

The synergistic enhancement that results from the alloying of Pd with Au has been well-reported in the literature, with the electronic modification of Pd species through the formation of nanoalloys, as well as disruption of contiguous Pd ensembles often attributed as the cause for the improved reactivity of bimetallic formulations, compared to monometallic analogues[19,25,26]. In particular, a growing number of studies have identified the improved performance of mixed domains of Pd<sup>2+</sup>-Pd<sup>0</sup> towards H<sub>2</sub>O<sub>2</sub> production, compared to Pd<sup>2+</sup>- or Pd<sup>0</sup>-rich surfaces[27–30].

Analysis of the as-prepared AuPd catalysts via XPS corroborates these earlier studies (Figure S.4), with a dramatic shift in Pd oxidation

state, towards Pd<sup>2+</sup> observed upon the introduction of Au into Pd, highlighting the extent of electronic modification possible, through the formation of bimetallic nanoalloys. Here we wish to highlight the presence of PdClx species in addition to PdO and Pd<sup>0</sup> present in these as-prepared materials, which is in keeping with earlier works into similarly prepared AuPd-based catalysts[24]. However, it should be noted that metal speciation within the fresh materials will not fully represent those present under reaction conditions, particularly given the relatively high partial pressures of H<sub>2</sub> utilised within the chemo-enzymatic cascade system.

Building on these initial studies, we subsequently investigated the efficacy of the chemo-catalytic formulations, when used in tandem with horseradish peroxidase (HRP) towards the polymerisation of phenol (Fig. 1, Table 2). Perhaps as expected based on our determination of initial rates of H<sub>2</sub>O<sub>2</sub> synthesis (Table 1), the 0.5 %Au–0.5 %Pd/TiO<sub>2</sub> catalyst was found to significantly outperform its monometallic and alternative bi-metallic analogues, achieving total conversion of phenol within 15 minutes of reaction (Fig. 1.A). Here we highlight that we do not observe any residual H<sub>2</sub>O<sub>2</sub> in the presence of HRP, which may indicate the potential for the reaction to be limited by chemo-catalytic H<sub>2</sub>O<sub>2</sub> production rate.

Clearly, this is a highly dynamic system, with both chemo-catalysed

**Table 2**

Comparison of chemo-enzymatic phenol polymerisation catalytic activity towards the polymerisation of phenol.

Catalyst	Reaction rate / mmol <sub>phenol</sub> conv. mmol <sub>metal</sub> <sup>-1</sup> *h <sup>-1</sup>	Phenol conversion / %**
1 %Au/TiO <sub>2</sub>	7.56 × 10 <sup>1</sup>	32
0.75 %Au–0.25 % Pd/TiO <sub>2</sub>	1.44 × 10 <sup>2</sup>	74
0.5 %Au–0.5 %Pd/TiO <sub>2</sub>	1.66 × 10 <sup>2</sup>	100
0.25 %Au–0.75 % Pd/TiO <sub>2</sub>	5.63 × 10 <sup>1</sup>	39
1 %Pd/TiO <sub>2</sub>	2.55 × 10 <sup>1</sup>	20

Chemo-enzymatic phenol polymerisation reaction conditions: chemo-catalyst (0.001 g), HRP (4U mL<sup>-1</sup>) phenol (0.3 mM), phosphate buffer (50 mM, 10 mL, pH8.0), using a gas mixture of 80 % H<sub>2</sub>/air (23 psi H<sub>2</sub>, 6 psi air), 20 °C, 0.25 h, 250 rpm. \*Reaction rate calculated at 10 % phenol conversion. \*\*Phenol conversion and residual HRP activity measurements are reported after a reaction time of 15 min.

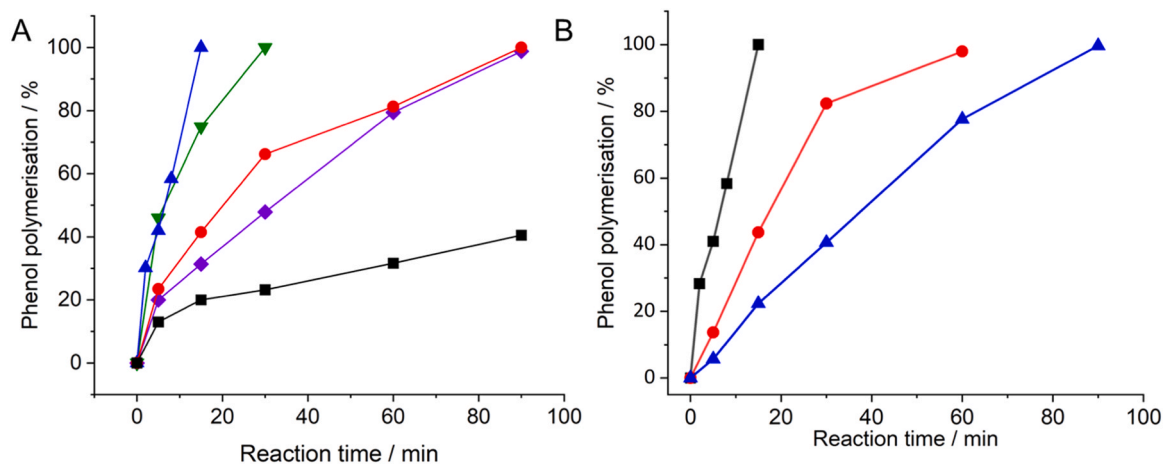


**Fig. 1.** A. The catalytic activity of 1 %AuPd/TiO<sub>2</sub> catalysts, when used in conjunction with HRP, towards the conversion of phenol. Key for Fig. 1. A: 1 %Au/TiO<sub>2</sub> (black squares), 0.75 %Au–0.25 %Pd/TiO<sub>2</sub> (red circles), 0.5 %Au–0.5 %Pd/TiO<sub>2</sub> (blue triangles), 0.25 %Au–0.75 %Pd/TiO<sub>2</sub> (inverted green triangles) and 1 %Pd/TiO<sub>2</sub> (purple diamonds). B. The performance of the 0.5 %Au–0.5 %Pd/TiO<sub>2</sub>/HRP chemo-enzymatic system towards phenol polymerisation, as a function of phenol concentration. Key for Fig. 1. B: 0.3 mM phenol (black squares), 0.6 mM phenol (red circles), 1.2 mM phenol (blue triangles). Chemo-enzymatic phenol polymerisation reaction conditions: chemo-catalyst (0.001 g), HRP (4 U mL<sup>-1</sup>) phenol (0.3–1.2 mM), phosphate buffer (50 mM, 10 mL, pH8.0), using a gas mixture of 80 % H<sub>2</sub>/air (23 psi H<sub>2</sub>, 6 psi air), 20 °C, 250 rpm.



H<sub>2</sub>O<sub>2</sub> synthesis and competitive degradation rates, as well as enzymatic activity varying throughout the reaction. However, our determination of initial H<sub>2</sub>O<sub>2</sub> production rate can be considered a relatively good metric to predict overall cascade performance (Tables 1 and 2) and indeed these measurements are promising given that Wang and co-workers have reported the Michaelis constant ( $K_m$ ) of HRP for H<sub>2</sub>O<sub>2</sub> as 3.7 mM [31]. These reports suggest that the AuPd catalysts investigated in this work would be active enough at ambient conditions to supply H<sub>2</sub>O<sub>2</sub> for HRP to catalyse phenol polymerisation, and also suggests that process efficiency would benefit from further improvements in catalytic rates of H<sub>2</sub>O<sub>2</sub> supply, again with the caveat that the H<sub>2</sub>O<sub>2</sub> production rate does not exceed that of its subsequent utilization by the enzyme.

A subsequent study, focussing on the optimal 0.5 %Au-0.5 %Pd/TiO<sub>2</sub> catalyst, in combination with HRP, revealed the efficacy of the chemo-enzymatic approach to phenol polymerisation, achieving total conversion of phenol, at a concentration four times that used within our standard studies, within a reaction time of 1.5 h (Fig. 1.B).

Interestingly, given earlier reports into the oxidative degradation of phenol via in-situ H<sub>2</sub>O<sub>2</sub> synthesis over Pd-based catalysts[2,32], no substrate conversion was observed in the absence of HRP (*i.e.* via a purely chemo-catalytic pathway) (Table S.2), which may be explained by the relatively large conditions gap that exists between this study and prior works into in-situ phenol oxidation. Indeed, these prior works also established the limited activity of Pd and AuPd-based catalysts towards phenol oxidation, especially compared to alternative formulations, such as PdFe[33]. Subsequently, over 2 h of reaction, and focussing on the 0.5 %Au-0.5 %Pd/TiO<sub>2</sub> chemo-catalyst, we established a significant improvement in phenol conversion may be achieved via the in-situ production of H<sub>2</sub>O<sub>2</sub> when coupled with HRP, in comparison to that observed when either gaseous reagent (H<sub>2</sub> and O<sub>2</sub> (as air)) is used separately (Table S.2), with no detectable conversion when using a purely reductive or oxidative atmosphere. Interestingly significantly higher rates of phenol polymerisation were also achieved via the in-situ production of H<sub>2</sub>O<sub>2</sub> (100 % within 15 min of reaction over the 0.5 % Au-0.5 %Pd/TiO<sub>2</sub> catalyst as reported in Fig. 1.A) compared to that obtained when using the preformed oxidant (13–89 % over 2 h), at comparable concentrations to that generated by the chemo-catalyst (from 20 – 100 ppm).

Comparison of HRP residual activity when the oxidant is supplied via in-situ chemo-catalytic synthesis or using ex-situ H<sub>2</sub>O<sub>2</sub>, at identical rates of phenol conversion, further highlights the improved performance of the in-situ approach (Table S.3). Indeed, the improved stability of the enzyme during the in-situ synthesis of the oxidant is notable and may be attributed to the continual supply of low-levels of H<sub>2</sub>O<sub>2</sub>, rather than the complete addition of H<sub>2</sub>O<sub>2</sub>, at the start of the reaction in the case of the ex-situ H<sub>2</sub>O<sub>2</sub> experiment. However, the potential detrimental role of H<sub>2</sub>O<sub>2</sub> stabilising agents (often a mixture of organic acids)[34] must also be considered, as must the potential for the HRP to become immobilised on the chemo-catalytic surface in the case of the in-situ H<sub>2</sub>O<sub>2</sub> experiments, this is particularly noteworthy given the often enhanced stability of immobilised enzymes, compared to their free analogues[35]. Using an ABTS assay, we next determined the contribution of key reaction parameters towards enzyme deactivation during the chemo-enzymatic polymerisation of phenol (Table 3). A considerable loss in enzyme activity was observed after exposure to reaction conditions, with the exposure of the enzyme to relatively mild pressures (29 psi), and the presence of the organic substrate (phenol) found to contribute significantly toward enzyme deactivation.

For any one-pot multi-step catalytic transformation to operate at maximum efficiency, there is clearly a need to balance rates of individual reaction pathways (*i.e.* the rate of chemo-catalytic H<sub>2</sub>O<sub>2</sub> synthesis and subsequent enzymatic utilisation of the oxidant), which is particularly challenging given the propensity of the chemo-catalysts to degrade H<sub>2</sub>O<sub>2</sub> (via hydrogenation and decomposition pathways) (Figure S.5). However, unlike with multi-functional chemo-catalytic approaches, there is also added complexity associated with the narrow operational

**Table 3**

The effect of reaction conditions on the activity of HRP, as determined by ABTS activity assays.

Conditions	HRP activity / U mL <sup>-1</sup>	Activity lost / %
HRP*	1.10	-
HRP + buffer + 250 rpm**	1.00	9
HRP + buffer + 250 rpm + H <sub>2</sub> + O <sub>2</sub>	0.83	25
HRP + buffer + 250 rpm + H <sub>2</sub> + O <sub>2</sub> + TiO <sub>2</sub>	0.91	17
HRP + buffer + 250 rpm + H <sub>2</sub> + O <sub>2</sub> + phenol	0.86	22
HRP + buffer + 250 rpm + N <sub>2</sub> + AuPd	0.96	13
HRP + buffer + 250 rpm + AuPd + H <sub>2</sub> + O <sub>2</sub>	0.74	33
HRP + buffer + 250 rpm + N <sub>2</sub> + AuPd + phenol	0.58	47

ABTS assay reaction conditions: 20  $\mu$ L of the reaction solution was added to 980  $\mu$ L ABTS solution (100 mM phosphate buffer, pH 6 with 0.3 mM ABTS and 2 mM H<sub>2</sub>O<sub>2</sub>) and substrate conversion was followed by measuring the absorption at 418 nm ( $\epsilon_{418} = 36000 \text{ M}^{-1} \text{ cm}^{-1}$ ) at 30 °C.\*HRP used as supplied. \*\* Reaction conducted at atmospheric pressure. Phenol polymerisation reaction conditions: Chemo-catalyst / TiO<sub>2</sub> (0.001 g), phenol (0.3 mM), HRP (1 U mL<sup>-1</sup>), phosphate buffer (10 mL, pH 6.0, 100 mM), total pressure (29 psi), 250 rpm, 20 °C, 1.5 h. Note 1: For experiments carried out using gaseous reagents pressures of H<sub>2</sub> (23 psi) and air (6 psi) or N<sub>2</sub> (29 psi) were used. Note 2: AuPd is indicative of 0.5 %Au-0.5 %Pd/TiO<sub>2</sub> catalyst.

window of the enzymatic component and limited stability of the synthesised H<sub>2</sub>O<sub>2</sub> under near-ambient conditions (*i.e.* in the absence of the low-temperatures, alcohol co-solvents and halide promoters often used to promote catalytic selectivity towards H<sub>2</sub>O<sub>2</sub>)[36]. With a focus on the 0.5 %Au-0.5 %Pd/TiO<sub>2</sub> chemo-catalytic formulation, and in an attempt to both further understand the chemo-enzymatic system and improve overall process efficiency, we subsequently investigated the role of key reaction parameters on phenol polymerisation.

Earlier studies into the HRP-mediated polymerisation of phenol utilising preformed H<sub>2</sub>O<sub>2</sub> have identified the relatively broad pH range in which the free enzyme is active (pH 6–8)[37]. By comparison, H<sub>2</sub>O<sub>2</sub> stability is well known to be favoured under acidic conditions[36]. Evaluation of chemo-catalytic synthesis of H<sub>2</sub>O<sub>2</sub> as a function of reaction solution pH is reported in Fig. 2.A, with an increased concentration of H<sub>2</sub>O<sub>2</sub> observed under more acidic reaction conditions. However, we wish to highlight that this is the net concentration of the oxidant produced, and in the case of the chemo-enzymatic system, one can expect the as-synthesised H<sub>2</sub>O<sub>2</sub> to be rapidly utilised by HRP, thus limiting the contribution of competitive chemo-catalytic H<sub>2</sub>O<sub>2</sub> degradation pathways. Subsequent screening of the chemo-enzymatic conversion of phenol, as a function of reaction solution pH, is reported in Fig. 2. B, with further data highlighting the negligible role of buffer concentration on process efficiency (at pH 8), in Figure S.6. Based on measurements of H<sub>2</sub>O<sub>2</sub> synthesis, as determined at a reaction time of 5 minutes and in the absence of HRP and phenol (Fig. 2.A), one may have expected improved rates of phenol conversion under a more acidic pH. However, no significant variation in phenol conversion can be observed over the pH range studied (pH 6–8), with approximately 40 % phenol conversion achieved at a reaction time of 10 minutes and 95 % conversion achieved after a reaction time of 30 minutes, regardless of pH.

The sensitivity of chemo-enzymatic processes to the concentration of the chemo-catalytic components (*e.g.* leached metal species or support phase) has been previously described, with even minor variation in this metric leading to a significant loss in performance[3]. In the case of chemo-catalytic in-situ H<sub>2</sub>O<sub>2</sub> supplied processes, this can be related to a number of factors, including (i) variation in the rate of H<sub>2</sub>O<sub>2</sub> supply and utilisation, (ii) immobilisation of the free enzyme onto the surface of the chemo-catalyst, (iii) enzymatic deactivation via interaction with leached metal species and (iv) the ability of any crude organic material present with the enzyme (or indeed the substrate or cascade reaction

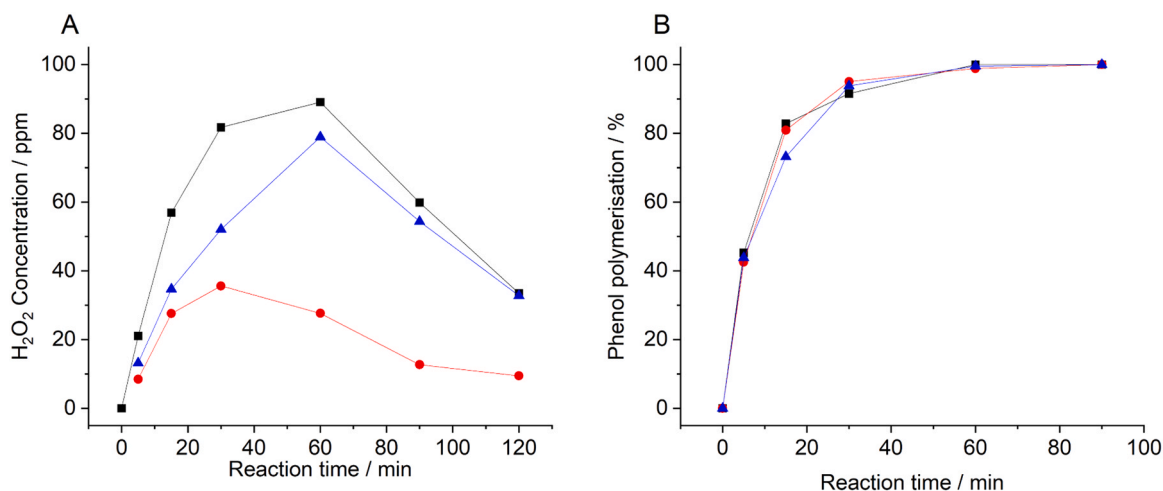


**Fig. 2.** The effect of reaction solution pH on (A) the direct synthesis of H<sub>2</sub>O<sub>2</sub> and (B) the chemo-enzymatic polymerisation of phenol, as a function of pH. Key for Fig. 2: pH 6 (black squares), pH 7 (red circles) and pH 8 (blue triangles). H<sub>2</sub>O<sub>2</sub> direct synthesis reaction conditions: Catalyst (0.001 g), phosphate buffer (100 mM, 10 mL), using a gas mixture of 80 % H<sub>2</sub>/air (23 psi H<sub>2</sub>, 6 psi air), 20 °C, 250 rpm. Chemo-enzymatic phenol polymerisation reaction conditions: chemo-catalyst (0.001 g), HRP (1 U mL<sup>-1</sup>) phenol (0.3 mM), phosphate buffer (100 mM, 10 mL), using a gas mixture of 80 % H<sub>2</sub>/air (23 psi H<sub>2</sub>, 6 psi air), 20 °C, 250 rpm.

products) to act as a sink for the synthesised H<sub>2</sub>O<sub>2</sub>. Investigation into the effect of chemo-catalytic concentration on H<sub>2</sub>O<sub>2</sub> synthesis rates (in the absence of the HRP enzyme and phenol substrate) is reported in Fig. 3.A, with corresponding measurements of chemo-enzymatic phenol polymerisation reported in Fig. 3.B. Interestingly, at short reaction times, where the extent of phenol conversion is relatively limited (< 70 %) there is a strong correlation between H<sub>2</sub>O<sub>2</sub> synthesis rate and phenol conversion (Table S.4).

Complimentary studies into the effect of HRP content are shown in Fig. 4, with an optimal HRP concentration of 4 U mL<sup>-1</sup> identified (100 % phenol conversion at a reaction time of 15 min), aligning well with our earlier studies into the chemo-enzymatic selective oxidation of cyclohexane, which utilised similar AuPd-based catalysts to those used in this work and the unselective peroxygenase, PaDa-I. Further increasing HRP content led to a considerable decrease in substrate conversion rate and a related improvement in residual enzyme stability [38]. Such an observation is particularly interesting and may be attributed to the ability of

the enzyme (or associated organic matter), to (i) deactivate chemo-catalytic H<sub>2</sub>O<sub>2</sub> synthesis through deposition onto the AuPd/TiO<sub>2</sub> catalyst or (ii) to act as a sink for the synthesised oxidant. Although one must also consider the possibility of product-mediated deactivation of the enzyme. Likewise, HRP-mediated H<sub>2</sub>O<sub>2</sub> decomposition via catalase-like pathways are also considered contributing factors to the apparent loss in process efficiency [39].

Regardless, given the relative cost of the purified enzyme, it is important to highlight that for this technology to be adopted at a larger scale there is a need to maximise enzyme lifetime (which can be inferred from measurements of residual enzyme activity in this work). In niche applications this may be achieved by the introduction of co-solvents [40]. This is clearly not applicable for application in the disinfection of potable water. However, the use of an immobilized enzyme would allow for improved enzymatic lifetimes and operation in a continuous/semicontinuous mode (likely necessary for use in water disinfection). Indeed, given that, alongside H<sub>2</sub>O<sub>2</sub>-mediated inactivation of

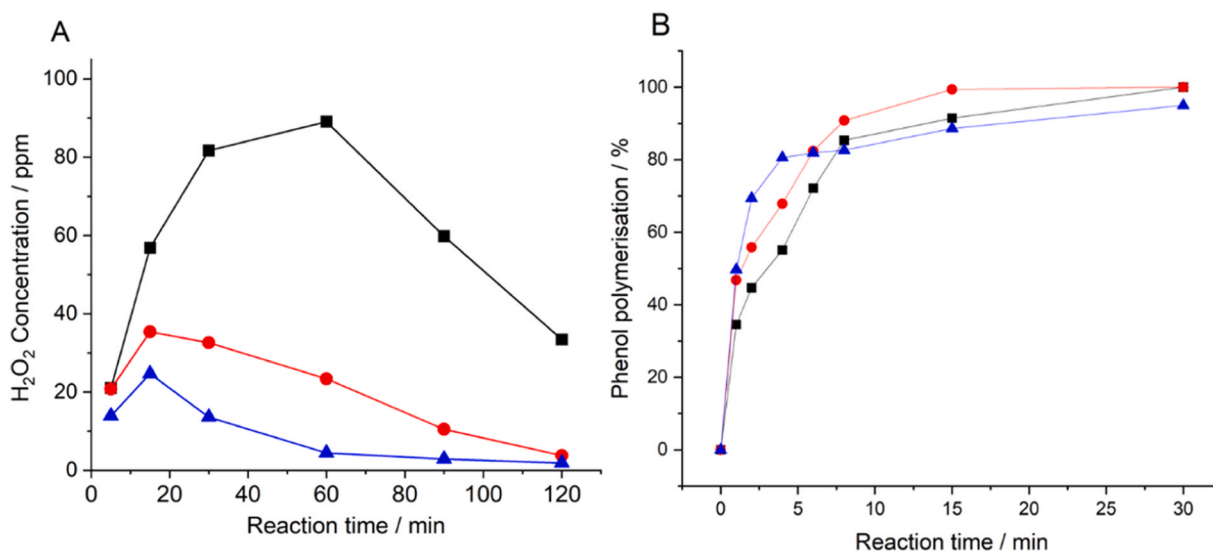


**Fig. 3.** The effect of catalyst mass on the (A) direct synthesis of H<sub>2</sub>O<sub>2</sub> and (B) the chemo-enzymatic polymerisation of phenol. Key: 1 mg (black squares), 2 mg (red squares) and 4 mg (blue triangles). H<sub>2</sub>O<sub>2</sub> direct synthesis reaction conditions: catalyst (0.001 g), phosphate buffer (50 mM, 10 mL, pH8.0), using a gas mixture of 80 % H<sub>2</sub>/air (23 psi H<sub>2</sub>, 6 psi air), 20 °C, 250 rpm. Chemo-enzymatic phenol polymerisation reaction conditions: catalyst (0.001 g), HRP (1 U mL<sup>-1</sup>) phenol (0.3 mM), phosphate buffer (50 mM, 10 mL, pH8.0), using a gas mixture of 80 % H<sub>2</sub>/air (23 psi H<sub>2</sub>, 6 psi air), 20 °C, 250 rpm.

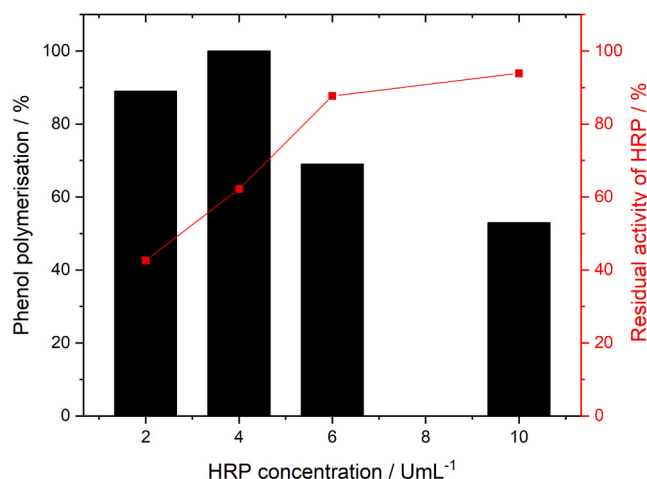


**Fig. 4.** The effect of HRP concentration on chemo-enzymatic polymerisation of phenol. Reaction conditions: chemo-catalyst (0.001 g), HRP (2–10 U mL<sup>-1</sup>) phenol (0.3 mM), phosphate buffer (50 mM, 10 mL, pH 8.0), using a gas mixture of 80 % H<sub>2</sub>/air (23 psi H<sub>2</sub>, 6 psi air), 20 °C, 250 rpm, 15 min.

the heme-centre, HRP deactivation via adsorption onto polymeric products is a major route to HRP activity loss [38], there are clear benefits of a flow-type, rather than batch, operation mode, where standing concentrations of both synthesised H<sub>2</sub>O<sub>2</sub> and products can be controlled.

As such alternative approaches to improve enzyme stability are recommended, and we consider that the development of composite materials that consist of both the chemo-catalytic and enzymatic components is treated as a priority of future studies.

To probe these potential pathways to process deactivation, H<sub>2</sub>O<sub>2</sub> synthesis studies were conducted in the presence of the enzyme (and the absence of phenol) (Figure S.7), along with complimentary H<sub>2</sub>O<sub>2</sub> decomposition studies in the absence of the chemo-catalyst (Figure S.8). Collectively, these data suggest that competitive HRP-mediated H<sub>2</sub>O<sub>2</sub> degradation pathways are a likely source of process inefficiency in the chemo-enzymatic process.

The potential for homogeneous metal species to contribute towards enzymatic deactivation has been previously reported [3]. With this earlier study in mind, we next set out to establish the effect of leached metals on HRP stability. However, the relatively low mass of the catalyst (0.001 g) and metal loadings (1 wt% total), used in this study dictated the use of model leaching studies in order to determine the extent of precious metal leaching during the chemo-enzymatic cascade (Table S.5). Such studies were conducted in the absence of both the HRP enzyme and the phenol substrate and at catalyst loadings (0.01 g) ten times greater than that utilised for our standard studies to allow for more accurate determination of leached metal concentrations. Notably, total metal leaching was found to be relatively limited (0.03 % for both Au and Pd). Building on this data, further model experiments were conducted in order to determine the role of leached metal species on enzyme stability. These experiments were conducted in the presence of the HRP enzyme and using a broad range of metal concentrations (Table S.6).

**Table 4**

Catalyst reusability in the chemo-enzymatic polymerisation of phenol, when used in conjunction with HRP.

Reaction number	Reaction rate / mmol <sub>phenol</sub> conv. <sup>-1</sup> mmol <sub>metal</sub> h <sup>-1</sup>	Phenol polymerisation / %	H <sub>2</sub> O <sub>2</sub> synthesis initial reaction rate / mmol <sub>H<sub>2</sub>O<sub>2</sub></sub> mmol <sub>metal</sub> h <sup>-1</sup> *	H <sub>2</sub> O <sub>2</sub> Concentration / ppm (mM)
1	1.28 × 10 <sup>2</sup>	100	7.88 × 10 <sup>2</sup>	21 (0.62)
2	1.18 × 10 <sup>2</sup>	92.5	9.00 × 10 <sup>2</sup>	24 (0.71)
3	1.15 × 10 <sup>2</sup>	90.4	7.13 × 10 <sup>2</sup>	19 (0.56)

Chemo-enzymatic phenol polymerisation reaction conditions: catalyst (0.001 g), HRP (4 U mL<sup>-1</sup>) phenol (0.3 mM), phosphate buffer (50 mM, 10 mL, pH 8.0), using a gas mixture of 80 % H<sub>2</sub>/air (23 psi H<sub>2</sub>, 6 psi air), 20 °C, 0.25 h, 250 rpm. H<sub>2</sub>O<sub>2</sub> direct synthesis reaction conditions: Chemo-catalyst (0.001 g), phosphate buffer (100 mM, 10 mL, pH 6.0), using a gas mixture of 80 % H<sub>2</sub>/air (23 psi H<sub>2</sub>, 6 psi air), 20 °C, 250 rpm. \*Initial reaction rate measured at 5 minutes of reaction.

Interestingly, unlike our earlier work which focussed on the combination of AuPd-based chemo-catalysts with the unspecific peroxygenase PaDa-I, we did not observe a meaningful loss in enzymatic activity through exposure to precious metals or indeed to the chloride counter ion. Such observations are promising and highlight the considerable variation in enzymatic tolerance to homogeneous metal species.

We next evaluated catalytic performance towards the direct synthesis of H<sub>2</sub>O<sub>2</sub> and the tandem chemo-catalytic-enzymatic polymerisation of phenol over multiple uses (Table 4), utilising fresh enzyme for each reaction. Such experiments allow for the stability of the chemo-catalytic component to be understood and indeed suggest that there is only a minor loss in the performance of the heterogeneous catalyst upon reuse, with phenol conversion remaining over 90 % over the course of three successive reactions. The observed loss in performance can, at least in part, be related to variation in catalytic activity towards H<sub>2</sub>O<sub>2</sub> production, however, other factors cannot be fully ruled out.

Subsequently, we evaluated the stability of the one-pot chemo-enzymatic system as a whole. Our earlier observations (Fig. 1.B), established that, when starting with an initial phenol concentration of 0.3 mM, it was possible to achieve total phenol polymerisation at a reaction time of 15 minutes, utilising a HRP concentration of 4 U mL<sup>-1</sup> and 0.001 g of the chemo-catalyst. Building on these experiments, fresh reagents (phenol (0.3 mM), H<sub>2</sub> (23 psi) and O<sub>2</sub> as air (6 psi)), were reintroduced to the reactor once total phenol polymerisation has been achieved (*i.e.* after a reaction time of 15 minutes, Fig. 5). It was possible to again achieve total conversion of the substrate. However, it was necessary to extend the reaction beyond that required in the first cycle (100 % phenol polymerisation at 30 minutes after the introduction of fresh reagents). While this may be attributed to the observed loss in

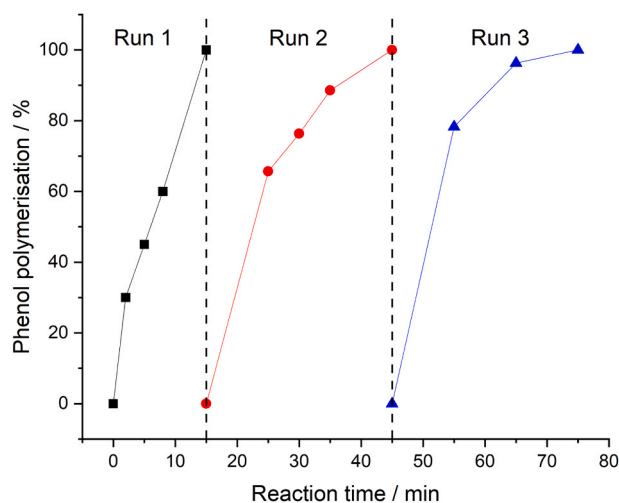


**Fig. 5.** Stability of the chemo-enzymatic system, over successive phenol polymerisation reactions. Key: dashed lines indicate substrate (phenol, H<sub>2</sub> and O<sub>2</sub>) recharging. Chemo-enzymatic phenol polymerisation reaction conditions: catalyst (0.001 g), HRP (4 U mL<sup>-1</sup>) phenol (0.3 mM), phosphate buffer (50 mM, 10 mL, pH 8.0), using a gas mixture of 80 % H<sub>2</sub>/air (23 psi H<sub>2</sub>, 6 psi air), 20 °C, 250 rpm.

chemo-catalytic performance (as indicated by the data reported in Table 4), it is also important to note the potential for enzymatic deactivation, through exposure to the phenol substrate (reported in Table 3) and polymeric products[38]. After a total of 45 minutes of reaction, liquid and gaseous reagents were again reintroduced. The system was again able to achieve total phenol polymerisation after an additional 30 minutes of reaction, which may indicate that process deactivation is not associated with the build of reaction products and instead may be related to the loss of chemo-catalytic performance over extended reaction times.

#### 4. Conclusions

The combination of a H<sub>2</sub>O<sub>2</sub> synthesizing chemo-catalyst and horseradish peroxidase has been shown to be highly effective in the oxidative polymerization of phenol, achieving rates of substrate conversion considerably higher than that observed when using preformed, commercial H<sub>2</sub>O<sub>2</sub>, representing an attractive alternative to co-enzymatic systems or the continual introduction of preformed oxidant. The introduction of Au into supported Pd nanoparticles is seen to considerably improve cascade activity compared to monometallic analogues, as a result of improved H<sub>2</sub>O<sub>2</sub> synthesis, with the high efficacy through combination of the 0.5 %Au-0.5 %Pd/TiO<sub>2</sub> catalyst with the HRP enzyme largely retained upon successive uses of the chemo-catalyst.

We have also identified the potential for enzymatic deactivation under cascade reaction conditions, primarily through exposure to the phenol substrate. Interestingly, the extent of enzyme deactivation through exposure to homogeneous metals, a concern that has previously been identified for alternative peroxidase-type enzymes, was found to be limited. We consider such observations will aid in further process design and optimisation, in particular, it is recommended that focus is placed on the immobilisation of the free enzyme, either directly onto the chemo-catalyst or onto secondary carriers, in order to both improve enzymatic stability but also to allow for operation in continuous/semi-continuous reactor systems.

We consider that the process developed within this study represents a promising basis for further investigation, particularly for the remediation of phenolic derivatives and other contaminants found in waste streams.

#### Funding

L.Z. acknowledges the Chinese Scholarship Council for funding. R.J.L, J.B, and G.J.H gratefully acknowledge Cardiff University and the Max Planck Centre for Fundamental Heterogeneous Catalysis (FUNCAT) for financial support. R.J.L, J.B and G.J.H also acknowledge financial support from UKRI (EP/V044060/1). Y.W is grateful to the National Natural Science Foundation of China (22325204) for their financial support.

#### CRediT authorship contribution statement

**Brehm Joseph:** Writing – original draft, Supervision, Methodology, Investigation, Data curation. **Liu Wencong:** Writing – review & editing, Writing – original draft, Investigation. **Morgan David:** Writing – review & editing, Methodology, Funding acquisition, Formal analysis, Data curation. **Davies Thomas:** Writing – review & editing, Methodology, Formal analysis, Data curation. **Wang Yong:** Writing – review & editing, Supervision, Project administration, Funding acquisition. **Hutchings Graham John:** Writing – review & editing, Supervision, Project administration, Methodology, Funding acquisition, Conceptualization. **Zhang Liwei:** Writing – original draft, Validation, Formal analysis, Data curation. **Lewis Richard:** Writing – review & editing, Writing – original draft, Supervision, Project administration, Methodology, Formal analysis, Conceptualization.

#### Declaration of Competing Interest

The authors declare that they have no known competing financial interests or personal relationships that could have appeared to influence the work reported in this paper.

#### Acknowledgements

XPS data collection was performed at the EPSRC National Facility for XPS (“HarwellXPS”), operated by Cardiff University and UCL, under contract no. PR16195. The authors would like to thank the CCI-Electron Microscopy Facility which has been part-funded by the European Regional Development Fund through the Welsh Government and The Wolfson Foundation.

#### Author contributions

L.Z., J.B and R. J. L. conducted catalytic synthesis, testing and data analysis. L.Z, R. J. L., W.L., D. J. M. and T. E. D. conducted catalyst characterisation and corresponding data processing. R. J. L. and G. J. H. contributed to the design of the study. R. J. L., J.B, Y.W and G. J. H. provided technical advice and result interpretation. R. J. L. wrote the manuscript and ESI, with all authors commenting on and amending both documents. All authors discussed and contributed to the work.

#### Dedication

This paper is dedicated to Prof. Ted Oyama in recognition of his receiving the George A. Olah Award in Hydrocarbon or Petroleum Chemistry and his many seminal contributions to the field.

#### Appendix A. Supporting information

Supplementary data associated with this article can be found in the online version at [doi:10.1016/j.cattod.2025.115292](https://doi.org/10.1016/j.cattod.2025.115292).

#### Data Availability

Data will be made available on request.

#### References

- [1] T. Richards, J.H. Harry, R.J. Lewis, A.G.R. Howe, G.M. Suldecki, A. Folli, D. J. Morgan, T.E. Davies, E.J. Loveridge, D.A. Crole, J.K. Edwards, P. Gaskin, C. J. Kiely, Q. He, D.M. Murphy, J. Maillard, S.J. Freakley, G.J. Hutchings, A residue-free approach to water disinfection using catalytic in situ generation of reactive oxygen species, *Nat. Catal.* 4 (2021) 575–585.
- [2] A. Santos, R.J. Lewis, D.J. Morgan, T.E. Davies, E. Hampton, P. Gaskin, G. J. Hutchings, The oxidative degradation of phenol via in situ H<sub>2</sub>O<sub>2</sub> synthesis using Pd supported Fe-modified ZSM-5 catalysts, *Catal. Sci. Technol.* 12 (2022) 2943–2953.
- [3] A. Stenner, R.J. Lewis, J. Brehm, T. Qin, Á. López-Martín, D.J. Morgan, T.E. Davies, L. Chen, X. Liu, G.J. Hutchings, Chemo-enzymatic one-pot oxidation of cyclohexane via in-situ H<sub>2</sub>O<sub>2</sub> production over supported AuPdPt catalysts, *ChemCatChem* 15 (10) (2023) e202300162.
- [4] D. Wilbers, J. Brehm, R.J. Lewis, J. van Marwijk, T.E. Davies, D.J. Morgan, D. J. Opperman, M.S. Smit, M. Alcalde, A. Kotsiopoulos, S.T.L. Harrison, G. J. Hutchings, S.J. Freakley, Controlling product selectivity with nanoparticle composition in tandem chemo-biocatalytic styrene oxidation, *Green. Chem.* 23 (2021) 4170–4180.
- [5] Y. Ma, Y. Li, S. Ali, P. Li, W. Zhang, M.C.R. Rauch, S.J. Willot, D. Ribitsch, Y. H. Choi, M. Alcalde, F. Hollmann, Y. Wang, Natural deep eutectic solvents as performance additives for peroxygenase catalysis, *ChemCatChem* 12 (2020) 989–994.
- [6] V. Smeets, W. Baaziz, O. Ersen, E.M. Gaigneaux, C. Boissière, C. Sanchez, D. P. Debecker, Hollow zeolite microspheres as a nest for enzymes: a new route to hybrid heterogeneous catalysts, *Chem. Sci.* 11 (2020) 954–961.
- [7] P.N.R. Vennestrom, E. Taarning, C.H. Christensen, S. Pedersen, J. Grunwaldt, J. M. Woodley, Chemoenzymatic Combination of Glucose Oxidase with Titanium Silicalite-1, *ChemCatChem* 2 (2010) 943–945.
- [8] F. Tieves, S.J. Willot, M.M.C.H. vanSchie, M.C.R. Rauch, S.H.H. Younes, W. Zhang, J. Dong, P. GomezdeSantos, J.M. Robbins, B. Bommarius, M. Alcalde, A. S. Bommarius, F. Hollmann, Formate oxidase (FOx) from *aspergillus oryzae*: one



- catalyst enables diverse H<sub>2</sub>O<sub>2</sub>-dependent biocatalytic oxidation reactions, *Angew. Chem. Int. Ed.* 58 (2019) 7873–7877.
- [9] E.G. Hryciay, S.M. Bandiera, The monooxygenase, peroxidase, and peroxygenase properties of cytochrome P450, *Arch. Biochem. Biophys.* 522 (2012) 71–89.
- [10] R.J. Lewis, K. Ueura, X. Liu, Y. Fukuta, T. Qin, T.E. Davies, D.J. Morgan, A. Stenner, J. Singleton, J.K. Edwards, S.J. Freakley, C.J. Kiely, L. Chen, Y. Yamamoto, G. J. Hutchings, Selective ammoxidation of ketones via in situ H<sub>2</sub>O<sub>2</sub> synthesis, *ACS Catal.* 13 (2023) 1934–1945.
- [11] Q. Liu, J.H. Lunsford, Controlling factors in the direct formation of H<sub>2</sub>O<sub>2</sub> from H<sub>2</sub> and O<sub>2</sub> over a Pd/SiO<sub>2</sub> catalyst in ethanol, *Appl. Catal., A* 314 (2006) 94.
- [12] M. Aurioi, Y. Filali-Meknassi, C.D. Adams, R.D. Tyagi, Natural and synthetic hormone removal using the horseradish peroxidase enzyme: Temperature and pH effects, *Water Res* 40 (2006) 2847–2856.
- [13] M. Aurioi, Y. Filali-Meknassi, R.D. Tyagi, C.D. Adams, Oxidation of natural and synthetic hormones by the horseradish peroxidase enzyme in wastewater, *Chemosphere* 68 (2007) 1830–1837.
- [14] W. Zheng, L.M. Colosi, Peroxidase-mediated removal of endocrine disrupting compound mixtures from water, *Chemosphere* 85 (2011) 553–557.
- [15] L.M. Colosi, Q. Huang, W.J. Weber, Quantitative structure–activity relationship based quantification of the impacts of enzyme–substrate binding on rates of peroxidase-mediated reactions of estrogenic phenolic chemicals, *J. Am. Chem. Soc.* 128 (2006) 4041–4047.
- [16] E. Miland, M.R. Smyth, C.Ó. Fágáin, Phenol removal by modified peroxidases, *J. Chem. Technol. Biotechnol.* 67 (1996) 227–236.
- [17] W. Cheng, W.F. Harper, Chemical kinetics and interactions involved in horseradish peroxidase-mediated oxidative polymerization of phenolic compounds, *Enzym. Microb. Technol.* 50 (2012) 204–208.
- [18] J.K. Edwards, B. Solsona, E. Ntainjua N, A.F. Carley, A.A. Herzing, C.J. Kiely, G. J. Hutchings, Switching off hydrogen peroxide hydrogenation in the direct synthesis process, *Science* 323 (2009) 1037.
- [19] N.M. Wilson, P. Priyadarshini, S. Kunz, D.W. Flaherty, Direct synthesis of H<sub>2</sub>O<sub>2</sub> on Pd and AuPd clusters: Understanding the effects of alloying Pd with Au, *J. Catal.* 357 (2018) 163.
- [20] R.J. Lewis, K. Ueura, Y. Fukuta, S.J. Freakley, L. Kang, R. Wang, Q. He, J. K. Edwards, D.J. Morgan, Y. Yamamoto, G.J. Hutchings, The direct synthesis of H<sub>2</sub>O<sub>2</sub> Using TS-1 supported catalysts, *ChemCatChem* 11 (2019) 1673.
- [21] J.K. Edwards, A.F. Carley, A.A. Herzing, C.J. Kiely, G.J. Hutchings, Direct synthesis of hydrogen peroxide from H<sub>2</sub> and O<sub>2</sub> using supported Au–Pd catalysts, *Faraday Discuss.* 138 (2008) 225.
- [22] S.J. Freakley, S. Kochius, J. van Marwijk, C. Fenner, R.J. Lewis, K. Baldenius, S. S. Marais, D.J. Opperman, S.T.L. Harrison, M. Alcalde, M.S. Smit, G.J. Hutchings, A chemo-enzymatic oxidation cascade to activate C–H bonds with in situ generated H<sub>2</sub>O<sub>2</sub>, *Nat. Commun.* 10 (2019) 4178.
- [23] J. Brehm, R.J. Lewis, T. Richards, T. Qin, D.J. Morgan, T.E. Davies, L. Chen, X. Liu, G.J. Hutchings, Enhancing the chemo-enzymatic one-pot oxidation of cyclohexane via in situ H<sub>2</sub>O<sub>2</sub> production over supported Pd-based catalysts, *ACS Catal.* (2022) 11776–11789.
- [24] T. Richards, R.J. Lewis, D.J. Morgan, G.J. Hutchings, The direct synthesis of hydrogen peroxide over supported Pd-based catalysts: an investigation into the role of the support and secondary metal modifiers, *Catal. Lett.* (2022).
- [25] F. Menegazzo, M. Manzoli, M. Signoretto, F. Pinna, G. Strukul, H<sub>2</sub>O<sub>2</sub> direct synthesis under mild conditions on Pd–Au samples: Effect of the morphology and the composition of the metallic phase, *Catal. Today* 248 (2015) 18–27.
- [26] J. Brehm, R.J. Lewis, D.J. Morgan, T.E. Davies, G.J. Hutchings, The direct synthesis of hydrogen peroxide over AuPd nanoparticles: an investigation into metal loading, *Catal. Lett.* 152 (2022) 254–262.
- [27] D.W. Flaherty, Direct synthesis of H<sub>2</sub>O<sub>2</sub> from H<sub>2</sub> and O<sub>2</sub> on Pd catalysts: current understanding, outstanding questions, and research needs, *ACS Catal.* 8 (2018) 1520.
- [28] F. Wang, C. Xia, S.P. de Visser, Y. Wang, How Does the Oxidation State of Palladium Surfaces Affect the Reactivity and Selectivity of Direct Synthesis of Hydrogen Peroxide from Hydrogen and Oxygen Gases? A Density Functional Study, *J. Am. Chem. Soc.* 141 (2019) 901–910.
- [29] L. Ouyang, P.-f. Tian, G. Da, X. Xu, C. Ao, T. Chen, R. Si, J. Xu, Y. Han, The origin of active sites for direct synthesis of H<sub>2</sub>O<sub>2</sub> on Pd/TiO<sub>2</sub> catalysts: Interfaces of Pd and PdO domains, *J. Catal.* 321 (2015) 70–80.
- [30] X. Gong, R.J. Lewis, S. Zhou, D.J. Morgan, T.E. Davies, X. Liu, C.J. Kiely, B. Zong, G.J. Hutchings, Enhanced catalyst selectivity in the direct synthesis of H<sub>2</sub>O<sub>2</sub> through Pt incorporation into TiO<sub>2</sub> supported AuPd catalysts, *Catal. Sci. Technol.* 10 (2020) 4635.
- [31] A. Santos, R.J. Lewis, D.J. Morgan, T.E. Davies, E. Hampton, P. Gaskin, G. J. Hutchings, The degradation of phenol via in situ H<sub>2</sub>O<sub>2</sub> production over supported Pd-based catalysts, *Catal. Sci. Technol.* 11 (2021) 7866–7874.
- [32] L. Wu, G. Wan, N. Hu, Z. He, S. Shi, Y. Suo, K. Wang, X. Xu, Y. Tang, G. Wang, Synthesis of Porous CoFe<sub>2</sub>O<sub>4</sub> and Its Application as a Peroxidase Mimetic for Colorimetric Detection of H<sub>2</sub>O<sub>2</sub> and Organic Pollutant Degradation, *Nanomaterials* 8 (2018) 451.
- [33] R. Underhill, R.J. Lewis, S.J. Freakley, M. Douthwaite, P.J. Miedziak, J.K. Edwards, O. Akdim, G.J. Hutchings, Oxidative Degradation of phenol using in-situ generated H<sub>2</sub>O<sub>2</sub> combined with Fenton’s process, *Johns. Matthey Technol. Rev.* 62 (2018) 417.
- [34] J.R. Scoville, I.A. Novicova (Cottrell Ltd.), US 5900256, 1996.
- [35] M.A.F. Delgove, D. Valencia, J. Solé, K.V. Bernaerts, S.M.A. De Wildeman, M. Guillén, G. Álvaro, High performing immobilized Baeyer-Villiger monooxygenase and glucose dehydrogenase for the synthesis of  $\epsilon$ -caprolactone derivative, *Appl. Catal. A* 572 (2019) 134–141.
- [36] A. Santos, R.J. Lewis, G. Malta, A.G.R. Howe, D.J. Morgan, E. Hampton, P. Gaskin, G.J. Hutchings, Direct Synthesis of Hydrogen Peroxide over Au–Pd Supported Nanoparticles under Ambient Conditions, *Ind. Eng. Chem. Res.* 58 (2019) 12623–12631.
- [37] G. Bayramoğlu, M.Y. Arica, Enzymatic removal of phenol and p-chlorophenol in enzyme reactor: Horseradish peroxidase immobilized on magnetic beads, *J. Hazard. Mater.* 156 (2008) 148–155.
- [38] L. Mao, S. Luo, m Q. Huang, J. Lu, Horseradish Peroxidase Inactivation: Heme Destruction and Influence of Polyethylene Glycol, *Sci. Rep.* 3 (2013) 3126.
- [39] J. Hernández-Ruiz, M.B. Arno, A.N.P. Hiner, F. García-Cánovas, M. Acosta, Catalase-like activity of horseradish peroxidase: relationship to enzyme inactivation by H<sub>2</sub>O<sub>2</sub>, *Biochem. J.* 354 (2001) 107–114.
- [40] T. Hilberath, A. van Troost, M. Alcalde, F. Hollmann, Assessing Peroxygenase-Mediated Oxidations in the Presence of High Concentrations of Water-Miscible Co-Solvents, *Front. Catal.* 2 (2022) 882992.